



A novel luminescent probe for ultrasensitive and label-free detection of morphine based on DNA-functionalized cerium oxide nanoparticles

Mostafa Sharafi¹, Masoomeh Shaghaghi^{2,*}, Nader Sheibani³, Gholamreza Dehghan^{1,*}

¹ Department of Biology, Faculty of Natural Sciences, University of Tabriz, Tabriz, Iran

² Department of Chemistry, Payame Noor University, P. O. Box 19395-4697 Tehran, Iran

³ Department of Ophthalmology and Visual Sciences, University of Wisconsin School of Medicine and Public Health, Madison WI 53705 USA

ARTICLE INFO

Article history:

Received 16 February 2024

Received in revised form 10 May 2024

Accepted 11 May 2024

Available online 15 May 2024

Keywords:

Optical biosensor

Fluorescence spectroscopy

Label-free methods

Morphine determination

Cerium oxide nanoparticles

ABSTRACT

A novel, fast, highly sensitive, and selective non-enzymatic label-free method was developed based on the fluorescence emission activity of surface-modified cerium oxide nanoparticles (CeO₂ NPs) for morphine (MP) detection. The fluorescence intensity of CeO₂ NPs increased following the adsorption of double-stranded DNA (dsDNA) onto its surface. Upon the addition of MP, the fluorescence intensity of the dsDNA-CeO₂ NPs probe switched to a “turn-off” state and was quenched. This was attributed to the binding of MP to dsDNA and displacement of dsDNA with MP from the NPs. Under optimized conditions (pH 7.4; dsDNA concentration 1.1×10⁻⁶ M and a time of 30 and 10 min for incubation of dsDNA with CeO₂ NPs and for MP and dsDNA-CeO₂ NPs incubation, respectively), the fluorescent sensor was able to detect MP with high sensitivity. A linear relationship was obtained in the range of [(3.5–35)×10⁻⁶ M] with a limit of detection (LOD) of 1.8×10⁻⁶ M and the relative standard deviation (RSD)% 1.5–2.3%. The proposed system was successfully applied to determine MP levels in human urine samples from spiked patients and healthy individuals after deproteinization with acetonitrile. The analytical recoveries for treated biological samples ranged from 99.1 to 103.1%. The excellent selectivity for MP compared to other substances (The common interfering species, such as codeine, amphetamine, and methamphetamine) with concentrations 10-fold higher than MP. In addition, the newly proposed method was based on an optical biosensor, as compared to most existing methods, providing advantages such as rapidity, simplicity, low cost, and high sensitivity, thus, making it a promising method for rapid and direct determination of MP in clinical samples.

1. Introduction

Morphine (MP) is an alkaloid and a phenolic compound. It is the main alkaloid of opium, which can disrupt the function of the central nervous system. Clinically, MP is often used to relieve chronic pain in patients, especially after surgery. MP can be abused by people to make them feel good resulting in addiction.

Also, MP could be used by athletes as an analgesic to reduce pain during prolonged exercise [1]. If consumed in excess, MP is toxic with many side effects, including decreased heart rate, central nervous system disorders, hallucinations, muscle tightening, and unwanted respiratory complications [2–4]. It is clinically important to accurately determine MP concentration in a patient’s urine or blood samples [1,2,5]. MP assessment is used to

* Corresponding author; e-mail: dehghan2001d@yahoo.com & gdehghan@tabrizu.ac.ir, m.shag2003d@yahoo.com & m_shaghaghi@pnu.ac.ir

<https://doi.org/10.22034/CRL.2024.444277.1297>



This work is licensed under Creative Commons license CC-BY 4.0

check for drug abuse and to identify the causes of poisoning or death for clinical and pathological intentions [2]. Thus, the quantitative measurement of MP is of significant clinical importance.

Various analytical methods have been used to detect MP levels such as high-performance liquid chromatography [6], spectrometry [7,8], immunoassay [9], and some electrochemical methods such as voltammetry and amperometry [10-19]. However, these techniques often have some disadvantages such as long sample pre-treatment steps, and they are lengthy with high costs.

The biosensors are frequently used in the detection and quantification of chemical or biochemical substances and pollutants, and various monitoring in biotechnology, medicine, and drug discovery [20-23]. Biosensors are defined as small/compact analytical devices that combine biological elements with an electronic component to generate measurable signals. A typical biosensor consists of an analyte (target), bioreceptor (biorecognition element), transducer, electronics, and display [20]. Optical biosensors, as a subset of biosensors, generate optical signals, which are directly proportional to the levels of the analyte. Common biorecognition elements used in optical biosensors are enzymes, nucleic acids, antibodies, antigens, receptors, and whole cells and tissues [20,24].

The most used optical biosensors are fluorescence, chemiluminescence, surface plasmon resonance (SPR), and surface-enhanced Raman scattering-based optical biosensors [20,24]. Optical biosensors present different advantages compared to traditional analytical techniques. They are fast, label-free, provide real-time measurements of analytes in biological samples with high specificity and reproducibility, and are cost-effective and biocompatible. Therefore, label-free methods are stable, simple, and inexpensive, have excellent detection ranges, and need small amounts of analyte for detection. In contrast, label-based methods are expensive, time-consuming, and complex. The sample pretreatments and preparations of the detection system are also tedious [24-27].

In recent years, fluorescence-based optical biosensors because of the noted advantages and less sensitivity to matrix effects have attracted increasing attention. These types of biosensors are most widely used for the determination of biological samples in clinical applications such as cancer monitoring and medical diagnosis. Various types of fluorescent materials, such as nanoparticles (carbon nanotubes and metal nanoparticles and quantum dots (QDs)), pigments, and fluorescent proteins, are used in these types of

biosensors. Fluorescent quenching (turn-off), fluorescent enhancement (turn-on), and fluorescence resonance energy transfer (FRET) are the three approaches used to assess changes in the specific use of these biosensors [20,24,28].

Cerium dioxide nanoparticles (CeO_2 NPs) or nanoceria, due to their unique and excellent chemical, physical, electronic, electrochemical, and optical properties have been used in various applications [29-32]. In addition, CeO_2 NPs have catalytic and antioxidant properties due to their ability to switch between oxidative states (Ce (IV) and Ce (III)), and the presence of these mixed-valence states on the surface. Thus, they could play an important role in scavenging some reactive nitrogen and oxygen species like superoxide and hydroxyl radicals, hydrogen peroxide, peroxynitrite, and nitric oxide [33-36]. Another characteristic of CeO_2 NPs is their luminescence emission, which has been the subject of numerous publications. Violet/blue luminosity has been reported from CeO_x and CeO_2 films [37,38]. Compared to other NPs, CeO_2 NPs crystalline form increases its optical, electrical, and structural properties due to its very small size and surface-to-volume increase [38,39].

In recent years, sensors based on DNA-functionalized metal oxide nanomaterials (MONMs), have been designed for sensing purposes as probes for specific targets and surface reactions. The combination of DNA with MONMs has greatly expanded bioassays [40]. In this regard, the adsorption of DNA oligonucleotides by a variety of MONMs, including CeO_2 has been studied [41,42]. As a result of the DNA, double-stranded (ds), or single-stranded (SS), interactions with the MONMs, probes based on fluorescence quenching and recovery have been developed. Thus, assays based on competitive adsorption with DNA on MONMs and DNA recognizing analytes and regulation of the nanozyme-activity of MONMs by DNA are performed [42]. DNA oligonucleotides can specifically bind a wide range of analytes making DNA use great potential in biological analysis and diagnostics [41-43].

By considering the advantages of optical biosensors and label-free methods as well as CeO_2 NPs, and important non-enzymatic assays, we report a new method for measuring low MP levels in biological samples. The technique used in this work to detect MP is spectrofluorimetry, a sensitive and powerful method for measuring analytes, especially drug analytes. The probe was designed with dsDNA decorated CeO_2 NPs, which are highly efficient and much less toxic than QDs and other fluorescent materials. In addition, there is no

need to change the surface and use an enzyme, which makes our method much more sensitive and faster than similar techniques for MP determinations. Also, this technique provides easy, low cost, a lower detection limit, a wider linear range, high stability and selectivity, and a simple detection procedure. Furthermore, compared with enzyme-based methods that suffer from several limitations [28], the proposed sensing system, due to its stable structure, low cost, and availability, presents the application of nanobiotechnology for efficient MP detection. This method is also relatively free from the common contaminants interfering with analyte species present in biological samples.

2. Materials and methods

2.1. Reagents

All reagents and solvents were used without further purification and were of analytical grade. Double distilled water was used during this work. HCl and NaOH were purchased from Merck (Darmstadt, Germany). Acetonitrile (HPLC grade) was purchased from Scharlau (Barcelona, Spain). CeO₂ stock solution (0.3×10^{-3} M) is prepared by dissolving a certain amount of its powder in double distilled water. DNA stock solution (2.2×10^{-6} M) was prepared by dissolving the appropriate amount of DNA in the buffer solution. The DNA oligonucleotides used here in this work were obtained from Bioneer Company (South Korea). The oligonucleotide sequences are shown below:

P1: 5'-CATAGCGGCAGGATCAGTTACAGTG-3'

P2: 5'-CACTGTAAGTATCCTGCCGCTATG-3'

Aqueous solutions of glucose, glycine, NaCl, KCl, CaCl₂·2H₂O, CuCl₂·2H₂O, FeCl₂·6H₂O, ZnSO₄, MnCl₂·4H₂O, and MgCl₂ (all from Merck, Darmstadt, Germany) were prepared. MP stock solution (35×10^{-6} M) was prepared in double distilled water. MP was purchased from the Hananteb Company (Khuzestan, Iran). The buffer solution was Tris (hydroxymethyl) aminomethane-hydrochloric acid (1.0×10^{-2} M), prepared by dissolving the desired amount of Tris-base (Merck, Germany) in 90 ml of water and adjusting pH to 7.4 with HCl and the volume was to 100 ml with double distilled water. Codeine, amphetamine, and methamphetamine standards were purchased from the Hananteb Company (Khuzestan, Iran). Healthy (negative) human and patient (positive) urine samples were obtained from the Bonab Health Center laboratory (Bonab, Iran). Working standard solutions were

prepared daily by serial dilution of stock standards in water.

2.2. Instrumentation

Fluorescence spectra and intensities were measured using a Jasco FP-750 spectrometer (Kyoto, Japan). This device is equipped with a thermostat cell holder at a constant temperature, and a temperature control system model ETC-272T, to measure fluorescence intensities and draw the relevant spectra. The excitation wavelength was adjusted to 280 nm ($\lambda_{ex} = 280$ nm) and fluorescence intensity was measured at 421 nm ($\lambda_{em} = 280$ nm). All measurements were performed using a thermostat cell holder at 25 ± 0.1 °C. The excitation and emission bandwidths were set at 10.0 and 5.0 nm, respectively. UV-visible spectrophotometer (T60, PG Instruments Ltd, Leicestershire, UK) using a 1.0 cm cell was used for plotting related absorption spectra.

2.3. Preparation of CeO₂ NPs

An aqueous solution of Ce(NO₃)₃·6H₂O (1.0 g in 10 mL) was basified with a 1.0 M NaOH solution, and a white precipitate of Ce(OH)₄ was obtained. After repeatedly washing the solid Ce(OH)₄ in water, the solution mixture was dried in a 50 °C oven. Ce(OH)₄ and urea (1.0 g), as fuel, were mixed and ground into a powder. After that, the residual solid was crushed and calcined in a high-temperature furnace for 5.0 hours at 400 °C [44].

2.4. Preparation of dsDNA solution

A mixture containing ssDNA P1 and P2 oligonucleotides was prepared in Tris solution (1.0×10^{-2} M). The solution was then placed at 95 °C for 10 min, and gently cooled to room temperature to ensure complete P1 and P2 annealing to dsDNA.

2.5. Preparation of dsDNA-CeO₂ NPs system

CeO₂ NPs solution (100 μL; 1.0×10^{-4} M) and dsDNA solution (50 μL; 1.1×10^{-6} M) were added to the Tris-HCl buffer solution (100 μL; 1.0×10^{-2} M) and kept at room temperature for 30 min. The solution was exposed to 25 ± 0.1 °C and the fluorescence intensity was measured at 421 nm with an excitation wavelength of 280 nm against a blank solution.

2.6. MP determinations

To determine MP levels, the following analytical method was used to construct the calibration curve. Different concentrations of MP [(3.5, 7.0, 14, 21, and 35) $\times 10^{-6}$ M] were added to 100 μL of CeO_2 NPs (1.0×10^{-4} M), 50 μL of dsDNA (1.1×10^{-6} M), and 100 μL of Tris-HCl (1.0×10^{-2} M) solutions. The mixed solutions were kept at room temperature for 10 min and the fluorescence intensity was measured using the excitation wavelength of 280 nm against the blank solution at 421 nm (I_f). A similar solution was prepared without MP, and its fluorescence intensity was measured at 421 nm (I_0). The decrease in fluorescence intensity of the dsDNA- CeO_2 NPs probe (ΔI_f) by MP was determined as:

$$\Delta I_f (\%) = (I_0 - I_f) / I_0 \times 100 \quad (1)$$

2.7. MP determination in human urine samples

The proposed sensing system was utilized to determine MP levels in spiked urine samples obtained from healthy (negative) and patient (positive) subjects after deproteinization with acetonitrile. For this purpose, 1.5 mL of acetonitrile was added to the 0.5 mL of urine samples, previously spiked with different concentrations of MP standard solution for final concentrations in the range of [(0.03-17.5) $\times 10^{-6}$] M. Each sample was vortexed for 2.0 min, centrifuged at 10,000 rpm for 5.0 min, and the supernatant was diluted to 5.0 mL with double distilled water. The 0.05 mL of this solution for the next measurement was then used based on the methods indicated in sections 2.5 and 2.6 to analyze MP levels. To assess the accuracy of the proposed method, known concentrations of MP standard solutions were added to healthy and patient urine samples before the pretreatment step, and total MP concentrations were then determined. The recovery values were calculated by dividing the value found by the added amount. The limit of detection (LOD) and relative standard deviation (RSD) values were calculated by applying the IUPAC definition [45]. RSD % was obtained using the formula $\text{RSD \%} = (S/X) \times 100$, where S is the standard deviation of the five analyses and X is the mean of the given values. The LOD was calculated as $3S_b/m$, where S_b is the standard deviation of the blank and m is the slope of the calibration curve.

3. Results and discussion

3.1. Chemical approaches in the synthesis of CeO_2 NPs

CeO_2 is a rare earth metal oxide that has been chemically investigated due to its remarkable properties such as photocatalytic activity, high surface area, and

antioxidant, antibacterial, and anticancer activities. These properties depend on particle size, morphology, and their biocompatible nature [46]. CeO_2 NPs are synthesized by various chemical techniques such as hydrothermal, mechanochemical, sonochemical, sol-gel, co-precipitation, and microemulsion. Among these methods, the hydrothermal synthesis technique is very important because it provides high purity and quality, low cost, good homogeneity, and morphology-controlled growth [46]. Here the CeO_2 NPs were prepared as described in section 2.3. XRD results indicated only the cubic fluorite phase of CeO_2 . No other impurities were detected and these patterns showed that the samples were of high purity (supporting information, Fig. S1) [44].

3.2. Interaction studies of dsDNA with CeO_2 NPs using fluorescence spectroscopy, and the possibility of MP determination based on the dsDNA- CeO_2 NPs probe

Previous studies have shown that CeO_2 NPs in crystal form have an inherent fluorescence emission. These NPs are known for their cubic crystal structure, optical transparency, high refractive capacity, catalytic activities, and thermal and chemical stability, which have been utilized in biomedical and analytical applications [47-50]. Figure 1 shows that a CeO_2 NP solution has an intense and narrow fluorescence emission band at 421 nm ($\lambda_{\text{ex}} = 280$ nm), and after adsorption of DNA on NPs, the fluorescence intensity increased ("turn on" process) [41,51]. DNA is a polyphosphate and can forcefully adsorb on various metal oxides, mostly through its phosphate backbone. Although the amount of adsorption affinity depends on the length of DNA, the DNA sequence does not play a significant role. The researchers' findings have shown that the tendency of different NPs, including AuNPs, AgNPs, CuNPs, and gold clusters, to bind to different bases on oligonucleotides is different. The affinity of CeO_2 NPs to bind to different nucleotides was also the same, and binding occurred in the anionic phosphate chain [52-54]. In general, the shorter the phosphate chain is (length of the oligonucleotide fragment) the higher the surface density of DNA on MONPs is. However, DNAs with shorter lengths were less stable and had less affinity to be absorbed (supporting information, Fig. S2) [55]. Therefore, to have high sensitivity and stability, a balance must exist between the affinity and the density of DNA on NPs by changing the length of DNA or changing the type of MONPs [42,55,56]. Based on the displacement assays, DNA bonded on MONPs (e.g.

CeO₂ NPs), in the presence of various phosphorus-containing species, may be displaced from the NP surface by competing with them [42]. In other words, substances that react with the phosphate backbone of DNA can cause the oligonucleotide to move away from the NPs surface.

Fluorescence quenching (“turn-off” process) is a process in which the intensity of fluorescence from a fluorophore is reduced. Several molecular interactions such as molecular rearrangement, energy transfer,

formation of the ground state complex, excited state reactions, and the collision process can be the cause of quenching. Figure 2 shows that as a result of the addition of MP to the dsDNA-CeO₂ NPs probe, and its binding to DNA, quenching, and reduction of the fluorescence intensity of CeO₂ NPs occurred. Therefore, it can be estimated that MP, as a potent benzyloisoquinoline alkaloid can interact with DNA, perhaps through attachment to a small DNA groove displacing it from the CeO₂ NPs surface resulting in fluorescence quenching.

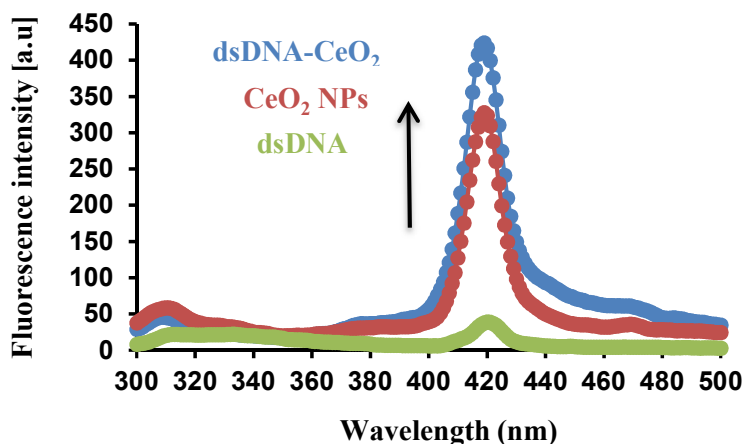


Fig. 1. Fluorescence emission spectra ($\lambda_{\text{ex}} = 280$ nm) of dsDNA, CeO₂ NPs, and dsDNA decorated CeO₂ NPs in aqueous solution. Conditions: $\lambda_{\text{em}} = 421$ nm, [CeO₂ NPs] = 1.0×10^{-4} M, [dsDNA] = 1.1×10^{-6} M, Tris-HCl = 0.01M and pH 7.4.

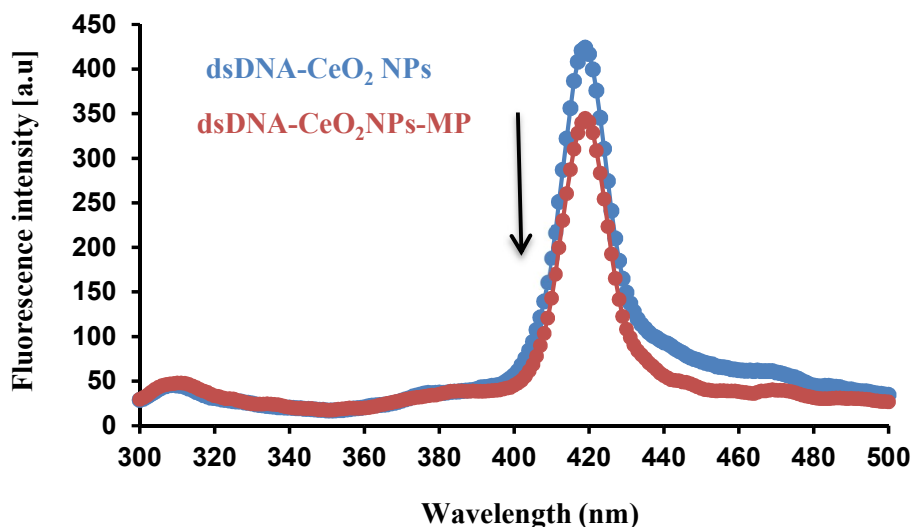


Fig. 2. Fluorescence emission spectra ($\lambda_{\text{ex}} = 280$ nm) of dsDNA-CeO₂ NPs probe in the presence of MP. Conditions: $\lambda_{\text{em}} = 421$ nm, [CeO₂ NPs] = 1.0×10^{-4} M, [dsDNA] = 1.1×10^{-6} M Tris-HCl = 0.01 M, and pH 7.4.

3.3. Optimization of experimental conditions

3.3.1. The effects of ssDNA and dsDNA

To evaluate the effect of ssDNA and dsDNA on the fluorescence intensity of the probe, both “turn on” and “turn off” processes, the results obtained from the two types of probes, dsDNA CeO₂ NPs and ssDNACeO₂, were compared (Fig. 3(A)). These results showed that

both dsDNA and ssDNA increased the fluorescence intensity of CeO₂ NPs. However, despite an increase in the fluorescence intensity of the CeO₂ NPs by ssDNA, the probe could not respond to the presence of MP in the environment by reducing the fluorescence intensity of the ssDNA-CeO₂ NPs probe. Thus, dsDNA was used to form a fluorescent probe.

3.3.2. The effect of DNA concentration

It is clear that many metal NPs have a negative charge at physiological pH with few exceptions, and DNA is strongly adsorbed on NPs. This adsorption is mostly in the phosphate backbone due to coordination with unsaturated metal surfaces or it is done electrostatically [55-57]. The effect of various dsDNA concentrations [(0.15-2.2)×10⁻⁶ M] on the fluorescence intensity of the probe was studied. Fig. 3(B) shows that with the addition of dsDNA the fluorescence intensity of CeO₂ NPs increased up to 1.1×10⁻⁶ M and higher DNA concentrations did not have additional effects on the fluorescence intensity. Thus, this DNA concentration was used to continue the process.

3.3.3. The effect of pH

Previous studies showed that the DNA adsorption on CeO₂ NPs is pH-dependent, and the adsorption increased to a certain pH value and then decreased [38]. In acidic pH, all MP molecules are cationic and can interact with the negative charge of the DNA phosphate backbone [43]. The experimental determination of MP levels has been often performed at near physiological pH (7-8) [29,31,43]. To find the optimum pH value, the effect of pH on the quenching efficiency [ΔI_f (%)] of the dsDNA CeO₂ prob was investigated in pH ranging from 5.4 to 9.4. Fig. 3(C) shows that the quenched fluorescence intensity of the probe reached a maximum at pH 7.4. Thus, pH 7.4 was selected as the optimal value.

3.3.4. The effect of incubation time

To study the effect of time on the increase of CeO₂ NPs fluorescence intensity due to dsDNA adsorption, under optimal conditions, fluorescence intensity was measured in four stages. The obtained results indicated that the fluorescence intensity of the CeO₂ NPs increased for up to 30 min, and then this increase took a steady trend (Fig. 3(D)). Also, by adding a constant concentration of MP to dsDNA-CeO₂ NPs, the effect of

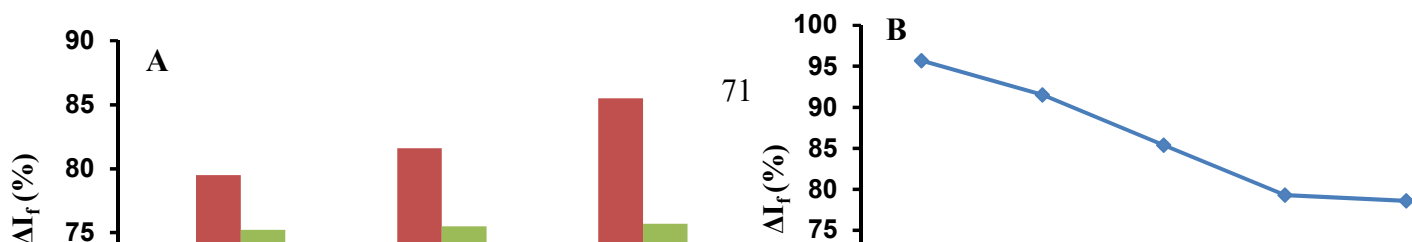
these times on the rate of reduction of fluorescence intensity of the dsDNA-CeO₂ NPs probe by MP was investigated. The value of ΔI_f (%) reached its maximum within the first 30 min and then decreased (Fig. 3(E)). Thus, a time of 30 minutes for incubation of DNA with CeO₂ NPs was selected.

To investigate the effect of MP incubation time on reducing the fluorescence intensity (fluorescence quenching) of the dsDNA-CeO₂ NPs probe, under optimal conditions, MP with constant concentration was added to the medium, and the fluorescence emission intensities were measured at specified intervals. These results showed that in the long incubation time, the quenching efficiency [ΔI_f (%)] of MP decreased (Fig. 3(F)). Thus, a time of 10 min for MP and dsDNA CeO₂ NPs incubation was selected.

3.4. Detection of MP using dsDNA-CeO₂ NPs probe

Considering the optimized conditions established above, the fluorescence response of the dsDNA-CeO₂ NPs probe to various MP concentrations was investigated, and a label-free spectrofluorimetric method was developed for MP detection. For this purpose, the effect of MP concentrations [(3.5-35)×10⁻⁶ M] on the fluorescence intensity of the dsDNA-CeO₂ NPs probe, under optimal conditions, was examined. With increasing MP concentration, the fluorescence intensity of the dsDNA-CeO₂ NPs probe switched to “turn off”. There was a linear relationship between the quenched fluorescence intensity of the probe and the MP concentration. This, suggests that MP binds the dsDNA releasing it from the surface of CeO₂ NPs (Fig. 4A). A calibration curve was drawn from the obtained results (Fig. 4B). The equation of the calibration curve is $\Delta I_f(\%) = 1.2982 C - 5.2813$ ($R^2 = 0.9895$), in which ΔI_f (%) is the quenched fluorescence intensity of the dsDNA-CeO₂ NPs probe by MP, and C is the MP concentration in M. The LOD, 1.8×10⁻⁶ M, was calculated. To evaluate the precision of the proposed method, a series of five solutions of 3.5, 7, and 14×10⁻⁶ M of MP were measured on the same day. The RSD for the five analyses was 1.5-2.3%.

The analytical features of the present method were compared with some of the methods used to detect MP in Table 1. As demonstrated, the proposed non-enzymatic method is very simple, fast, and low cost with high stability, accuracy, and sensitivity. Furthermore, special emission characteristics of CeO₂ NPs, such as narrow and strong emission bands, and



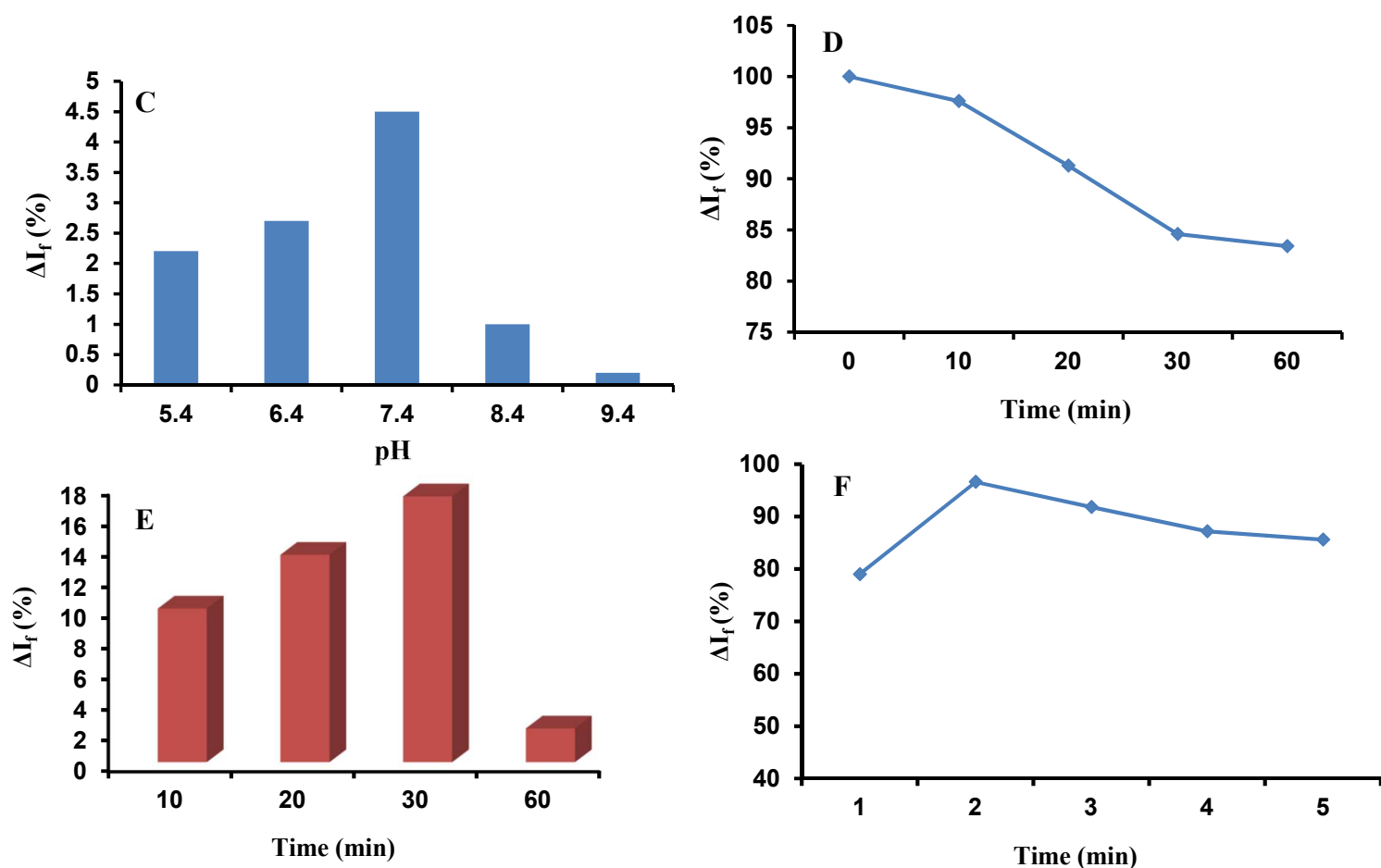


Fig. 3. (A) Comparison of the effect of ssDNA and dsDNA on the turn-on and turn-off fluorescence intensity of CeO₂ NPs; (a) The effect of ssDNA and dsDNA on the fluorescence intensity of CeO₂ NPs (turn-on process); (b) The effect of adding of MP on fluorescence intensity of dsDNA-CeO₂ NPs; (c) The effect of adding of MP on fluorescence intensity of ssDNA-CeO₂ NPs (turn-off process); (B) the effect of adding different concentrations of dsDNA on the fluorescence intensity of CeO₂ NPs; (C) The decrease of the fluorescence intensity of CeO₂ NPs with the addition of MP at different pH; (D) The effect of dsDNA and CeO₂ NPs incubation time on the fluorescence intensity of CeO₂ NPs; (E) The effect of dsDNA and CeO₂ NPs incubation time on reducing the fluorescence intensity of NPs in the presence of MP constant concentration in; (F) The effect of incubation time after adding MP constant concentration on reducing the fluorescence intensity of the dsDNA-CeO₂ NPs probe. Conditions: $\lambda_{em} = 421$ nm, $\lambda_{ex} = 280$ nm, [CeO₂ NPs] = 1.0×10^{-4} M, [dsDNA and ssDNA] = 1.1×10^{-6} M, [MP] = 7.0×10^{-6} M, Tris-HCl = 0.01 M and pH 7.4.

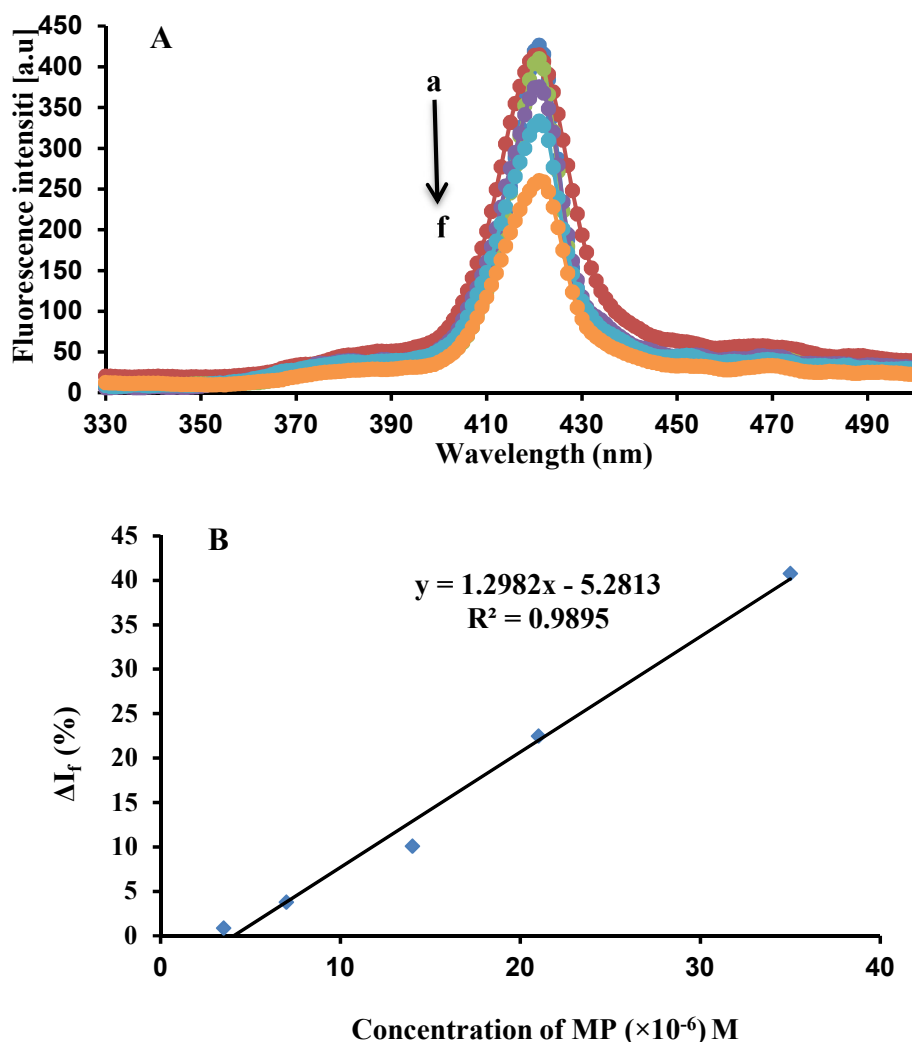


Fig. 4. (A) Fluorescence emission spectra ($\lambda_{\text{ex}} = 280 \text{ nm}$) of dsDNA-CeO₂ NPs system. Assay conditions: (a) dsDNA-CeO₂ NPs, ($[\text{CeO}_2 \text{ NPs}] = 1.0 \times 10^{-4} \text{ M}$, $[\text{dsDNA}] = 1.1 \times 10^{-6} \text{ M}$, $[\text{Tris-HCl}] = 0.01 \text{ M}$, and $\text{pH} = 7.0$); (b–f) dsDNA-CeO₂ NPs in the presence of increasing concentrations of MP; b = $3.5 \times 10^{-6} \text{ M}$, c = $7.0 \times 10^{-6} \text{ M}$, d = $14 \times 10^{-6} \text{ M}$, e = $21 \times 10^{-6} \text{ M}$ and f = $35 \times 10^{-6} \text{ M}$. (B) The corresponding calibration curve (The efficiency of fluorescence quenching, $\Delta I_f (\%) = (I_0 - I_f)/I_0 \times 100$ versus the concentration of MP). Conditions: $\lambda_{\text{em}} = 421 \text{ nm}$, $\lambda_{\text{ex}} = 280 \text{ nm}$, $[\text{CeO}_2 \text{ NPs}] = 1.0 \times 10^{-4} \text{ M}$, $\text{Tris-HCl} = 0.01 \text{ M}$, $\text{pH} = 7.4$, $[\text{dsDNA}] = 1.1 \times 10^{-6} \text{ M}$.

Table 1. The efficiency of the developed method compared to other methods reported for the detection of MP.

Modification method	Detection method	Linear range ($\times 10^{-6} \text{ M}$)	Detection limit ($\times 10^{-6} \text{ M}$)	Ref
Prussian blue film-modified palladized aluminum electrode	hydrodynamic amperometry	2-50	0.8	[19]
ZnO/CNT ^a nanocomposite ionic liquid modified carbon paste electrode	square wave voltammetry	0.1-700	0.06	[16]
Graphene/Pd/glassy carbon electrode	Electrochemical Method (DPV) ^b	0.34-12	0.01	[12]
Ordered mesoporous carbon-modified electrode	Electrochemical Method (CV) ^c	0.1-20	0.01	[13]

Multiwall carbon nanotubes paste electrode	square wave voltammetry	0.2-250	0.09	[17]
N-hexyl-3- methylimidazolium hexafluoro phosphate /multiwall carbon nanotubes paste electrode	differential pulse voltammetry	0.6–600	0.02	[18]
CdO nanoparticles, ionic liquid, carbon paste electrode	Electrochemical Method (SWV) ^d	0.5-800	0.1	[14]
Cobalt hexacyanoferrate /glassy carbon electrode	Electrochemical Method (DPV)	1– 50	0.5	[15]
dsDNA-CeO ₂ NPs	Fluorescence spectroscopy	3.5-35	1.8	This work

^a Zinc oxide/carbon nanotube

^b differential pulse voltammetric

^c Cyclic Voltammetry

^d Square Wave Voltammetry

also the important role of dsDNA in the stability of CeO₂ NPs and the specific bond of the analyte, are another advantage that allows the successful application of this method for the determining MP levels in real samples without the need for a separation technique.

3.5. Selectivity of the biosensor

To demonstrate the performance of the new MP fluorescent nanosensor, the selectivity of the proposed method was carried out with various common coexisting substances, such as codeine, amphetamine, and methamphetamine. The influence of interfering species was examined by the addition of increasing concentrations of these contaminants to the MP solution until a variation greater than 10% in fluorescence intensity was achieved. As shown in Table 2, changes in the relative fluorescence intensity of the dsDNA-CeO₂ NPs composite in the presence of MP were significantly larger than in other analytes, indicating that the proposed method shows high selectivity and can be used to detect MP in biological samples.

3.6. Detection of MP in human urine samples

To further investigate the application of this method as a fast, simple, reliable, and sensitive approach, the dsDNA-CeO₂ NPs probe was used as a “turn-off” fluorescence system to detect MP in urine samples using the method described in section 2.7. For this purpose, the fluorescence spectrum of the dsDNA-CeO₂ NPs probe with that of the dsDNA-CeO₂ NPs probe in the presence of an unspiked urine sample (blank) was studied. A comparison of these two spectra showed that the blank

had no effect on the fluorescence intensity of the dsDNA-CeO₂ NPs probe, and therefore the emission peak of the dsDNA-CeO₂ NPs probe at 421 nm could be

used to detect MP. There was a good linear relationship between MP concentration and fluorescence intensity in urine samples with MP in the range of [(3.5-35)×10⁻⁶ M] (R² = 0.992).

The accuracy of the method was evaluated by the added-found method and statistical treatment of MP determination data in the matrix.

Table 3 shows the results of MP analysis in spiked urine samples. The recoveries found for the urine sample and five replicates were in the range of 99.1-103.1%. and RSD in the range of 2.2-3.7%. Statistical analysis of the test results showed that the proposed method has acceptable accuracy and there was no significant difference between the reported and experimental results. These findings confirmed that the method performed here is simply due to the high sensitivity and selectivity of the system in urine samples without the need for a separation method, providing good accuracy, precision, and recovery. To further investigate the possibility of measuring this biosensor to detect MP in biological samples, urine samples of patients (MP addicts) were prepared from Bonab central laboratory, and MP levels in patients' urine were measured using the described calibration curve (Table 4). The obtained results were compared with those presented by Bonab Central Laboratory. These data demonstrated the practical application of the new sensor to detect MP in real clinical specimens.

Table 2. Tolerance limits of some interfering species in the determination of MP under optimal conditions.

Coexisting substance	Ratio of coexisting substance to morphine	ΔI_f (%)
Codeine	10:1	0.5
Amphetamine	10:1	0.3
Methamphetamine	10:1	0.35
Glucose	10:1	0.4
Glycine	10:1	0.38
Na ⁺	10:1	0.2
K ⁺	10:1	0.45
Ca ²⁺	10:1	0.25
Mg ²⁺	10:1	0.35
Fe ²⁺	10:1	0.3
Cu ²⁺	10:1	0.3
Mn ²⁺	10:1	0.35

$\Delta I_f\% = (F_1 - F_2) / F_2 \times 100$. Here, F_1 and F_2 are the fluorescence intensities of the systems with and without interferents, respectively.

Table 3. The application of the proposed method for the determination of MP in normal spiked urine samples with various MP concentrations.

Sample	Amount added ($\times 10^{-6}$ M) ^a	Amount found ($\times 10^{-6}$ M) ^b	Recovery (%)	RSD (%)
	3.5	3.52 \pm 0.03	100.5	2.2
	7.0	7.22 \pm 0.08	103.1	3.7
	14.0	13.94 \pm 0.91	99.1	2.4

^a Concentration values in final solutions

^b Average of five determinations \pm SD.

Table 4. Determination of MP concentration in patient urine samples using the dsDNA-CeO₂ NPs biosensor.

Patient samples	Found ($\times 10^{-6}$ M) ^a	Reference values ^b	RSD (%)
40 year-old-man	15.9 \pm 0.7	Positive	4.4
51 year-old-man	14.2 \pm 0.4	Positive	2.8
60 year-old-man	7.8 \pm 0.21	Positive	2.4
55 year-old-man	16.5 \pm 0.65	Positive	3.9

^a Value determined by the dsDNA-CeO₂ NPs probe, (average of five determinations \pm SD).

^b Value provided by Bonab central laboratory (TLC result cut-off value = 1.0×10^{-6} M).

4. Conclusion

We developed a fast, rapid, and highly sensitive biosensor for direct detection of MP in clinical samples using dsDNA decorated CeO₂ NPs as a fluorescent probe. This label-free and non-enzymatic sensor showed

sensitive and selective detection of MP, due to the unique characteristics of the dsDNA-CeO₂ NPs fluorescent probe. Our results showed that suitable linearity exists for detecting MP in the range of $[(3.5-35) \times 10^{-6}$ M] with a detection limit of 1.8×10^{-6} M. The presented procedure is very simple and superior to other

methods used to detect MP. The new strategy is free of any labeling process and without the need for additional charges in the dsDNA substrate or the minute design of the complex at room temperature.

References

- [1] A. Aliabadi, G.H. Rounaghi, A novel electrochemical sensor for determination of morphine in a sub-microliter of a human urine sample. *J. Electroanal. Chem.*, 832 (2019) 204-208.
- [2] V. Anitha Kumary, P. Abraham, S. Renjini, B.E. Kumara Swamy, T.E. Mary Nancy, A. Sreevalsan, A novel heterogeneous catalyst based on reduced graphene oxide supported copper coordinated amino acid – A platform for morphine sensing. *J. Electroanal. Chem.*, 850 (2019) 113367.
- [3] A. Navaee, A. Salimi, H. Teymourian, Graphene nanosheets modified glassy carbon electrode for simultaneous detection of heroin, morphine and noscipine. *Biosens. Bioelectron.*, 31(2012) 205-211.
- [4] G. Andersen, L. Christrup, P. Sjøgren, Relationships among morphine metabolism, pain and side effects during long-term treatment: an update. *J. Pain Symptom Manag.*, 25 (2003) 74-91.
- [5] M. Rajaei, M.M. Foroughi, S. Jahani, M. Shahidi Zandi, H. Hassani Nadiki, Sensitive detection of morphine in the presence of dopamine with La³⁺ doped fern-like CuO nanoleaves/MWCNTs modified carbon paste electrode. *J. Mole. Liq.*, 284 (2019) 462-472.
- [6] M. Jafari-Nodoushan, J. Barzin, H. Mobedi, A stability-indicating HPLC method for simultaneous determination of morphine and naltrexone. *J. Chromatogr. B Analyt. Technol. Biomed. Life Sci.*, 1011 (2016) 163-170.
- [7] R. Gottardo, A. Fanigliulo, F. Bortolotti, G. De Paoli, J. Paola Pascali, F. Tagliaro, Broad-spectrum toxicological analysis of hair based on capillary zone electrophoresis–time-of-flight mass spectrometry. *J. Chromatogr. A*, 1159 (2007) 190-197.
- [8] A. Sheibani, M. Reza Shishehbore, E. Mirparizi, Kinetic spectrophotometric method for the determination of morphine in biological samples. *Spectrochim. Acta A Mol. Biomol. Spectrosc.*, 77 (2010) 535-538.
- [9] D.J Chapman, S. P. Joel, G.W Aherne, Evaluation of a differential radioimmunoassay technique for the determination of morphine and morphine-6-glucuronide in human plasma. *J. Pharm. Biomed. Anal.*, 12 (1994) 353-360.
- [10] S. Barthwal, B. Singh, N.B. Singh, A novel electrochemical sensor fabricated by embedding ZnO nanoparticles on MWCNT for morphine detection. *Mat. Today: Proc.*, 5 (2018) 9061–9066.
- [11] G. Maccaferri, F. Terzi, Z. Xia F. Vulcano, A. Liscio, V. Palermo, C. Zanardi, Highly sensitive amperometric sensor for morphine detection based on electrochemically exfoliated graphene oxide. Application in screening tests of urine samples. *Sens. Actuators B Chem.*, 281 (2019) 739-745.
- [12] N.F Atta, H.K. Hassan, A. Galal, Rapid and simple electrochemical detection of morphine on graphene–palladium-hybrid-modified glassy carbon electrode. *Anal. BioAnal. Chem.*, 406 (2014) 6933–6942.
- [13] F. Li, J. Song, C. Shan, D. Gao, X. Xu, L. Niu, Electrochemical determination of morphine at ordered mesoporous carbon modified glassy carbon electrode. *Biosens. Bioelectron.*, 25 (2010) 1408-1413.
- [14] S. Cheraghi, M.A. Taher, H. Karimi-Maleh, A novel strategy for the determination of paracetamol in the presence of morphine using a carbon paste electrode modified with CdO nanoparticles and ionic liquids. *Electroanalysis*, 28 (2016) 366-371.
- [15] F. Xu, M. Gao, L. Wang, T. Zhou, L. Jin, Jiye Jin, Amperometric determination of morphine on cobalt hexacyanoferrate modified electrode in rat brain microdialysates. *Talanta*, 58 (2002) 427-432.
- [16] A.L. Sanati, H. Karimi-Maleh, A. Badiie, P. Biparva, A. A. Ensafi, A voltammetric sensor based on NiO/CNTs ionic liquid carbon paste electrode for determination of morphine in the presence of diclofenac. *Mater. Sci. Eng. C Mater. Biol. Appl.*, 35 (2014) 379-385.
- [17] A. Mokhtari, H. Karimi-Maleh, A.A. Ensafi, H. Beitollahi, Application of modified multiwall carbon nanotubes paste electrode for simultaneous voltammetric determination of morphine and diclofenac in biological and pharmaceutical samples. *Sens. Actuators B Chem.*, 169 (2012) 96-105.
- [18] Ali A. Ensafi, Maedeh Izadi, B. Rezaei, H. Karimi-Maleh, N-hexyl-3-methylimidazolium hexafluoro phosphate/multiwall carbon nanotubes paste electrode as a biosensor for voltammetric detection of morphine. *J. Mol. Liq.*, 174 (2012) 42-47.
- [19] M.H. Pournaghi-Azar, A. Saadatirad, Simultaneous voltammetric and amperometric determination of morphine and codeine using a chemically modified-palletized aluminum electrode. *J. Electroanal. Chem.*, 624 (2008) 293-298.
- [20] V. Naresh, N. Lee, A Review on Biosensors and Recent Development of Nanostructured Materials-Enabled Biosensors. *Sensors*, 21 (2021) 1109.
- [21] M. Yousefnezhad1, M. Babazadeh, S. Davaran, A. Akbarzadeh, H. Pazoki-Toroudi, Preparation and *in-vitro* evaluation of PCL–PEG–PCL nanoparticles for doxorubicin-ezetimibe co-delivery against PC3 prostate cancer cell line. *Chem. Rev. Lett.*, 7 (2024) 159-172.
- [22] A. Ullah, S. Rasheed, I. Ali, N. Ullah, Plant mediated synthesis of CdS nanoparticles: Their characterization and application for photocatalytic degradation of toxic organic dye. *Chem. Rev. Lett.*, 4 (2021) 98-107.
- [23] A.K.O. Aldulaim, N.M. Hameed, T.A. Hamza, A.S. Abed, The antibacterial characteristics of fluorescent carbon nanoparticles modified silicone denture soft liner. *J. Nanostruct.*, 12 (2022) 774-781.

- [24] N. Bhalla, P. Jolly, N. Formisano, P. Estrelam, Introduction to biosensors. *Essays Biochem.*, 60 (2016) 1–8.
- [25] M.Y. Saleh, A.K.O. Aldulaimi, S.M. Saeed, A.H. Adhab, TiFe₂O₄@SiO₂-SO₃H: A novel and effective catalyst for esterification reaction. *Heliyon*, 10 (2024) e26286.
- [26] C.R. Taitt, G.P. Anderson, Evanescent wave fluorescence biosensors. *Biosens. Bioelectron.*, 20 (2005) 2470-2487.
- [27] S. Rashtbari, G. Dehghan, M. Amini, An ultrasensitive label-free colorimetric biosensor for the detection of glucose based on glucose oxidase-like activity of nanolayered manganese-calcium oxide. *Anal. Chim. Acta*, 1110 (2020) 98e108.
- [28] G. Dehghan, M. Shaghghi, P. Alizadeh, A novel ultrasensitive and non-enzymatic "turn-on-off" fluorescence nanosensor for direct determination of glucose in the serum: As an alternative approach to the other optical and electrochemical methods. *Spectrochim. Acta A Mole. Biomol. Spectrosc.*, 214 (2019) 459-468.
- [29] S. Ansari, M. Shahnawaze Ansari, N. Dev, S.P.Satsangee, CeO₂ nanoparticles based electrochemical sensor for an anti-anginal Drug. *Mater. Today: Proc.*, 18 (2019) 1210–1219.
- [30] J. Roh, S.H. Hwang, J. Jang, Dual-functional CeO₂:Eu³⁺ nanocrystals for performance-enhanced dye-sensitized solar cells. *ACS Appl. Mater. Interfaces*, 22 (2014) 19825–19832.
- [31] A. Umar, R. Kumar, M.S. Akhtar, G. Kumar, S.H. Kim, Growth and properties of well-crystalline cerium oxide (CeO₂) nanoflakes for environmental and sensor applications. *J. Colloid Interface Sci.*, 454 (2015) 61-68.
- [32] S. Yang, G. Li, G. Wang, L. Liu, D. Wang, L. Qu, Synthesis of highly dispersed CeO₂ nanoparticles on N-doped reduced oxide graphene and their electrocatalytic activity toward H₂O₂. *J. Alloys Compd.*, 688 (2016) 910-916.
- [33] A. Umar, T. Almas, A.A. Ibrahim, R. Kumar, M.S. AlAssiri, S. Baskoutas, M.S. Akhtar, An efficient chemical sensor based on CeO₂ nanoparticles for the detection of acetylacetone chemical. *J. Electroanal. Chem.*, 864 (2020) 114089.
- [34] F. Charbgoon, M.B. Ahmad, M. Darroudi, Cerium oxide nanoparticles: green synthesis and biological applications. *Int. J. Nanomed.*, 12 (2017) 1401–1413.
- [35] M. Nadeem, R. Khan, K. Afridi, A. Nadhman, S. Faisal, Z.U. Mabood, C. Hano, B.H. Abbasi, Green synthesis of cerium oxide nanoparticles (CeO₂ NPs) and their antimicrobial applications: A Review. *Int. J. Nanomed.*, 15 (2020) 5951–5961.
- [36] P. Nithya, M. Balaji, A. Mayakrishnan, C.D. Kumar, S. Rajesh, A. Surya, M. Sundrarajan, Ionic liquid functionalized biogenic synthesis of Ag-Au bimetal doped CeO₂ nanoparticles from *Justicia adhatoda* for pharmaceutical applications: Antibacterial and anti-cancer activities. *J. Photochem. Photobiol. B Biol.*, 202 (2020) 111706.
- [37] A.S. Razavian, S.M. Ghoreishi, A.S. Esmaily, M. Behpour, L.M.A. Monzon, J.M.D. Coey Simultaneous sensing of L-tyrosine and epinephrine using a glassy carbon electrode modified with nafion and CeO₂ nanoparticles. *Microchim. Acta*, 181 (2014) 1947–1955.
- [38] M. Yan, T. Mori, J. Zou, J. Drennan, Effect of grain growth on densification and conductivity of Ca-Doped CeO₂ electrolyte. *J. Am. Chem. Soc.*, 92 (2009) 2745-2750.
- [39] J. Malleshappa H. Nagabhushana, B. Daruka Prasad, S.C. Sharma, Y.S. Vidya, K.S. Anantharaju Structural, photoluminescence and thermoluminescence properties of CeO₂ nanoparticles. *Optik (Stuttg.)*, 27 (2016) 855-861.
- [40] W. Zhou, R. Saran, J. Li, Metal Sensing by DNA, *Chem. Rev.* 117, 12 (2017) 8272–8325.
- [41] B. Liu, J. Liu, Sensors and biosensors based on metal oxide nanomaterials. *Trends Anal. Chem.*, 121 (2019) 115690.
- [42] Q. He, Q. Wu, X. Feng, Z. Liao, W. Peng, Y. Liu, D. Peng, Z. Liu, M. Mo, Interfacing DNA with nanoparticles: Surface science and its applications in biosensing. *Int. J. Biol. Macromol.*, 151 (2020) 757-780.
- [43] B. Liu, J. Liu, A Comprehensive screen of metal oxide nanoparticles for DNA adsorption, fluorescence quenching, and anion discrimination. *ACS Appl. Mater. Interfaces*, 44 (2015) 24833–24838.
- [44] M. Amini, R. Hassandoost, Copper nanoparticles supported on CeO₂ as an efficient catalyst for click reactions of azides with alkynes. *Catal. Commun.*, 85 (2016) 13-16.
- [45] ICH Harmonised Tripartite Guideline, Validation of analytical procedures: text and methodology Q2 (R1), 2005.
- [46] Y.A. Syed Khadar, A. Balamurugan, V.P. Devarajan, R. Subramanian, Synthesis, characterization, and antibacterial activity of cobalt doped cerium oxide (CeO₂: Co) nanoparticles by using hydrothermal method. *J. Mater. Res. Technol.*, 8 (2019)267-274.
- [47] B. Choudhury, P. Chetri, A. Choudhury, Annealing temperature and oxygen vacancy- dependent variation of lattice strain, band gap and luminescence properties of CeO₂ nanoparticles. *J. Exp. Nanosci.*, 10 (2015) 103-114.
- [48] L. Li, H.K. Yang, B.K. Moon, Z. Fu, C. Guo, J.H. Jeong, S.S. Yi, K. Jang, H.S. Lee, Photoluminescence properties of CeO₂:Eu³⁺ nanoparticles synthesized by a sol-gel method. *J. Phys. Chem. C*, 113, 2 (2009) 610–617.
- [49] V. Seminko, P. Maksimchuk, I. Bepalova, A. Masalov, O. Viagin, E. Okrushko, N. Kononets, Y. Malyukin, Defect and intrinsic luminescence of CeO₂ nanocrystals. *Phys. Status Solidi*, 254 (1017) 1600488.
- [50] Z. Yang, H. Wu, J. Li. Slow light enhanced near infrared luminescence in CeO₂: Er³⁺, Yb³⁺ inverse opal photonic crystals. *J. Alloys Compd.*, 641 (2015) 127-131.
- [51] Q. Liu, C. Jin, Y. Wang, X. Fang, X. Zhang, Z. Chen, W. Tan, Aptamer-conjugated nanomaterials for specific

- cancer cell recognition and targeted cancer therapy. *NPG Asia Materials*, 6 (2014) e95.
- [52] H. Malekzad, P. Sahandi Zangabad, H. Mohammadi, M. Sadroddini, Z. Jafari, N. Mahlooji, S. Abbaspour, S. Gholami, M. Ghanbarpoor, R. Pashazadeh, A. Beyzavi, M. Karimi, M.R. Hamblin, Noble metal nanostructures in optical biosensors: basics, and their introduction to anti-doping detection. *Trends Anal. Chem.*, 100 (2018) 116-135.
- [53] D.L. Morris, DNA-bound metal ions: recent developments. *Bio. Mol. Concepts*, 5 (2014) 1437-1596.
- [54] R. Pautler, E.Y. Kelly, P.J. Jimmy Huang, J. Cao, B. Liu, J. Liu, Attaching DNA to nanoceria: regulating oxidase activity and fluorescence quenching. *ACS Appl. Mater. Interfaces*, 5, 15 (2013) 6820–6825.
- [55] A. Lopez, Y. Zhang, J. Liu, Tuning DNA adsorption affinity and density on metal oxide and phosphate for improved arsenate detection. *J. Colloid Interface Sci.*, 493(2017) 249-256.
- [56] L. Chen, B. Liu, Z.R. Xu, J. Liu, NiO Nanoparticles for exceptionally stable DNA adsorption and its extraction from biological fluids. *Langmuir*, 34, 31 (2018) 9314–9321.
- [57] X. Wang, A. Lopez, J. Liu, Adsorption of phosphate and polyphosphate on nanoceria probed by DNA oligonucleotides. *Langmuir*, 34, 26 (2018) 7899–7905.